A New Mouse Model of Inducible, Chronic Retinal Ganglion Cell Dysfunction Not Associated with Cell Death

Xu Yang, Tsung-Han Chou, Marco Ruggeri, and Vittorio Porciatti

Purpose. To develop a mouse model of inducible, chronic retinal ganglion cell (RGC) dysfunction not associated with cell death.

Methods. Eighteen C57BL/6J mice were longitudinally tested with pattern electroretinogram (PERG) and spectral-domain optical coherence tomography (OCT) before and after aspiration of the contralateral superior colliculus (SC), which removed terminals of optic tract axons and the superficial layers of the SC. At the 4-month end points, retinas were harvested for Brn3b immunostaining and BDNF immunoblotting.

Results. The PERG lost approximately 60% of its baseline amplitude ($P < 0.01$) within the first day after lesion, and remained at a reduced level over 4 months. At the end point, the density of Brn3b-positive RGCs was normal, but their nucleus size was reduced by approximately 24% ($P < 001$). OCT measurements showed thinning of the inner, but not outer, retina by approximately 9% ($P < 0.01$) starting 10 to 20 days after lesion. Retinal nerve fiber layer thickness was unchanged. At the end point, retinal homogenates showed a substantial overexpression of BDNF protein level.

Conclusions. Mechanical SC lesion in adult mice results in a rapid, chronic loss of RGC electrical responsiveness that is followed by cell shrinkage but not cell death. The SC-lesion mouse represents a new, inducible model that allows investigating stages and mechanisms of RGC dysfunction without the confounding effects of cell death that are common in the existing models of optic neuropathies and optic nerve lesions. (*Invest Ophthalmol Vis Sci.* 2013;54:1898–1904) DOI: 10.1167/iovs.12-11375

Glaucoma and optic nerve diseases are a family of disorders whose final common pathway is retinal ganglion cell (RGC) degeneration resulting in blindness. Mouse models of optic neuropathies are commonly used to investigate pathophysiologic mechanisms leading to cell death and to test new treatment modalities.[1,2] Increasing evidence in animal models of glaucoma shows that RGC death may be preceded by a relatively long stage of neuropathy that is associated with RGC dysfunction.[3–5] RGC dysfunction may be reversible.[6,7] Investigating RGC dysfunction preceding cell death thus may provide key information to understand how ailing neurons cope with stressful, potentially fatal, conditions. This information is necessary for specific, timely treatment of the stressful conditions to prevent cell death and even restore RGC function.

In current models of glaucoma and optic nerve diseases, dysfunctional RGCs, potentially recoverable, coexist with dying or dead RGCs, all of them contributing to loss of visual function. Under most circumstances, it is difficult to investigate visual loss associated with ailing RGCs from visual loss associated with dying or dead RGCs. Here we describe a mouse model of inducible, chronic RGC dysfunction that does not result in cell death. RGC dysfunction is caused by mechanical lesion of the superior colliculus (SC). It will be shown that this procedure causes a rapid, chronic reduction of RGC electrical responsiveness, as measured by pattern electroretinogram (PERG).[8,9] Loss of PERG signal is followed by thinning of inner retinal thickness and shrinkage of RGC bodies, but not RGC death, over at least 4 months. The model is relevant for studies of preventive strategies in optic neuropathies, including testing of neuroprotective drugs. Preliminary results of this study have been previously published in abstract form (Yang X, et al. *IOVS*. 2010;51:ARVO E-Abstract 5485; and Ref. 10).

Materials and Methods

Animals and Husbandry

This study was approved by the Animal Care and Use Committee at the University of Miami. All experiments were conducted according to the ARVO Statement for the Use of Animals in Ophthalmic and Vision Research. C57BL/6J mice purchased from Jackson Laboratory (Bar Harbor, ME) were kept in our Association for the Assessment and Accreditation of Laboratory Animal Care (AAALAC)-certified vivarium, using standard 12:12-hour light-dark cycle and fed with Grain-Based Diet (Lab Diet: 500, Opti-diet; LabDiet, St. Louis, MO). For the present study, 18 mice, 4 months old at baseline, were used. PERG and optical coherence tomography (OCT) were recorded before and after SC lesion over a period of 4 months under ketamine/xylazine anesthesia. At the 4-month end point, mice were euthanized by cervical dislocation and the retinas processed for RGC counts and brain-derived neurotrophic factor (BDNF) immunostaining.

Surgical Procedure

Mice were weighed and anesthetized with intraperitoneal injections (0.5–0.7 mL/kg) of a mixture of ketamine, 42.8 mg/mL, and xylazine, 8.6 mg/mL. Under sterile conditions, the bone overlying the right SC (0.5 mm lateral to the central suture, 2.9 mm posterior to the bregma) was drilled to aspirate a narrow column of cortical tissue and expose the SC.[11] Then the superficial layers of the SC were also removed by aspiration. A similar procedure was used for control mice, except that

From the Bascom Palmer Eye Institute, University of Miami Miller School of Medicine, Miami, Florida.

Supported by National Institutes of Health (NIH)-National Eye Institute RO1 EY019077, NIH Grant P30-EY014801, and an unrestricted grant to Bascom Palmer Eye Institute from Research to Prevent Blindness, Inc.

Submitted for publication November 26, 2012; revised January 25, 2013; accepted February 11, 2013.

Disclosure: **X. Yang**, None; **T.-H. Chou**, None; **M. Ruggeri**, None; **V. Porciatti**, None

Corresponding author: Vittorio Porciatti, Bascom Palmer Eye Institute, McKnight Vision Research Center, 1638 NW 10th Avenue, Room 201D, Miami, FL 33136; vporciatti@med.miami.edu.

Investigative Ophthalmology & Visual Science, March 2013, Vol. 54, No. 3

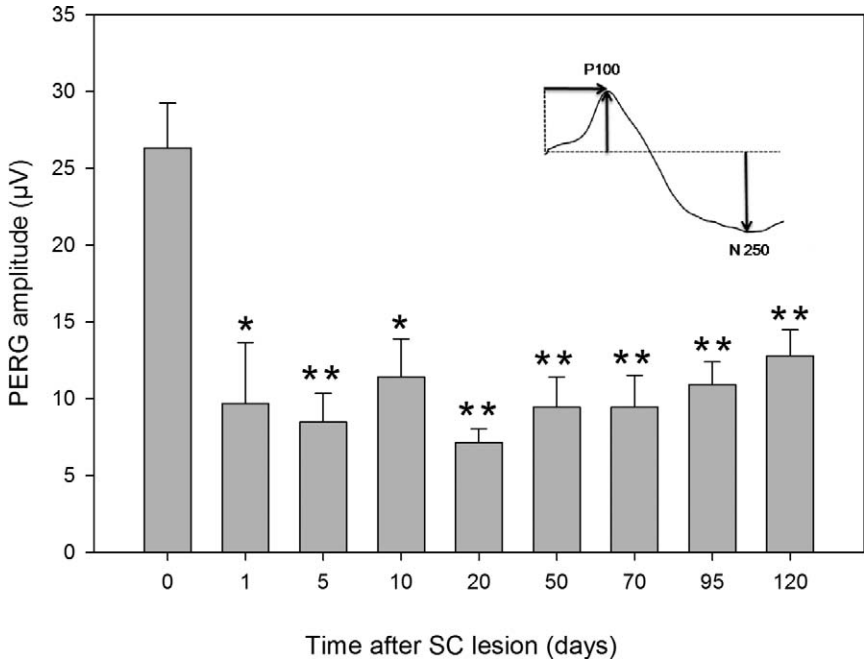

Figure 1. PERG amplitude before and at different times after lesion of the contralateral SC. Lesion was done on the right SC, and the PERG was recorded from the left eye. *Error bars* represent the SEM ($n = 18$). The *inset* shows a representative example of PERG response, whose amplitude was measured from the peak of the P100 wave to the trough of the N250 wave. *Asterisks above the bars* represent the level of significance compared to baseline ($^*P < 0.05$; $^{**}P < 0.01$).

the column of aspirated tissue was limited to cortical layers, leaving the SC intact. Mice were then allowed to recover from anesthesia and were put back in their cages. Surgical ablation of SC was preferred to lesions with neurotoxins, such as kainic acid or ibotenic acid[12] so as to exclude possible retrograde toxic effects to RGCs.

PERG Recording

Detailed description of the PERG technique is reported elsewhere.[7,9,13] In brief, mice were weighed and anesthetized with intraperitoneal injections (0.5–0.7 mL/kg) of a mixture of ketamine, 42.8 mg/mL, and xylazine, 8.6 mg/mL. Mice were then gently restrained in a custom-made holder that allowed unobstructed vision. The body of the animal was kept at a constant body temperature of 37°C by using a feedback-controlled heating pad (TCAT-2LVl; Physitemp Instruments, Inc., Clifton, NJ). The eyes of anesthetized mice were typically wide open and in a stable position, with optical axes pointing laterally and upwardly. A PERG electrode (0.25-mm diameter silver wire configured to a semicircular loop of 2-mm radius) was placed on the extrapupillary corneal surface by means of a micromanipulator. A small drop of balanced saline was topically applied every 30 minutes to prevent corneal dryness. Reference and ground electrodes were stainless steel needles inserted under the skin of the scalp on the back of the head and the tail, respectively. Visual stimuli consisted of contrast-reversing (2 reversal/s) horizontal bars (0.05 cyc/deg, 100% contrast, mean luminance 50 cd/m^2) generated by a programmable graphic card (VSG-Cambridge Research Systems, Rochester, UK) on a cathode-ray tube display (Sony Multiscan 500; Sony, Park Ridge, NJ) whose center was aligned with the projection of the pupil. The pupils were not dilated, and eyes were not refracted for the viewing distance, as the mouse eye has a large depth of focus.[14–16] At the viewing distance of 15 cm, the stimulus field covered an area of 69.4 × 63.4 degrees. Three consecutive PERG responses to 600 contrast reversals each were recorded. The responses were superimposed to check for consistency and then averaged (1800 sweeps). The PERG waveform consisted of a major positive peak at approximately 90 to 120 ms (defined as P100) followed by a slower negative wave with a broad trough at approximately 200 to 300 ms (defined as N250, examples in the inset of Fig. 1).[9,17] As a control for generalized effect of SC lesion to outer retinal neurons, a photopic ERG (FERG) was recorded in response to diffuse bright flashes on a rod-saturating background as previously described.[9] The FERG was recorded before and at the 4-month end point. The FERG waveform consisted of a major positive b-wave peaking at approximately 50 ms followed by a slower negative wave, also known as photopic negative response (PhNR).[9,18] The FERG amplitude was measured from the peak of the b-wave to the trough of the PhNR.

Spectral-Domain OCT

In vivo spectral-domain (SD)-OCT (Bioptigen, Inc., Durham, NC) images were performed before surgery and at different times thereafter over 4 months. Three-dimensional images were obtained from a raster of 100 b-scans centered on the optic disk and spanning an area of 1.3 × 1.3 mm^2. For the purpose of this study, three obvious landmarks were readily identified in b-scans of all tested mice: the retinal surface, the border between the inner nuclear layer (INL) and the outer plexiform layer (OPL), and the inner border of the pigment epithelium (PE). Inner retina was defined as the distance between the retinal surface and the border between INL and OPL. Outer retina was defined as the distance between the border between INL and OPL and the PE. A hollow cylinder of tissue (outer radius 0.65 mm, inner radius 0.2 mm) centered on the optic disk was analyzed. Retinal landmarks were manually identified on 100 b-scans spanning the entire tissue block and the average outer/inner retina thicknesses computed using custom software (examples in Fig. 2). Retinal nerve fiber layer (RNFL) was too thin to be identified in all slices and at all eccentricities. To measure RNFL thickness unambiguously, we manually analyzed a horizontal slice of tissue crossing the center of the optic disk and at an eccentricity of 275 μm for the disk center. At this eccentricity, the RNFL is sufficiently thick to allow reliable quantitative analysis.

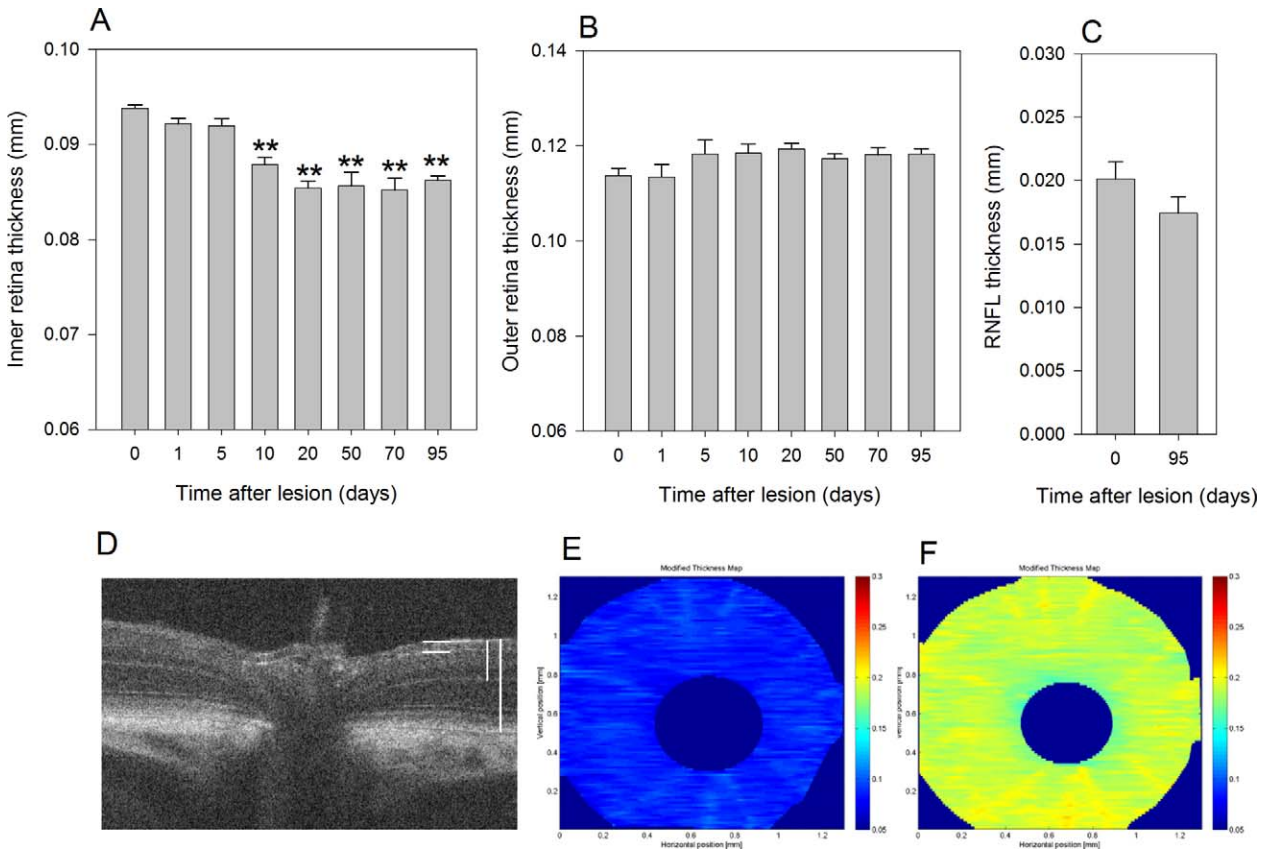

Figure 2. Mean thickness of different retinal layers before and after lesion of the contralateral SC. (**A**) Inner retina, (**B**) outer retina, (**C**) retinal nerve fiber layer (RNFL). *Error bars* represent the SEM ($n = 8$). *Asterisks above the gray bars* represent the level of significance compared with baseline (**$P < 0.01$). (**D**) Example of one OCT image intersecting the optic nerve head at its center. *Vertical bars* represent retinal layers that have been measured (*short bar*: inner retina; *longer bar*: total retina; *horizontal parallel bars*: retinal fiber layer). (**E**, **F**) Segmentation of inner retina thickness (**E**) compared with total retina thickness (**F**) for a hollow cylinder of tissue (outer radius 0.65 mm, inner radius 0.2 mm) centered on the optic disk. Images were obtained from a raster of 100 b-scans spanning an area of 1.3 × 1.3 mm centered on the optic disk. RNFL thickness was manually measured on a horizontal slice of tissue crossing the center of the optic disk and at an eccentricity of 275 μm for the disk center.

Immunohistochemistry for RGC Counts

At the 4-month end point, eyes ($n = 6$) were harvested and placed overnight in 4% EM-grade paraformaldehyde fixative (#15,710; Electron Microscopy Sciences, Hatfield, PA). Retinas were then dissected, rinsed in PBS (127 mM NaCl, 2.7 mM KCl, 10 mM phosphate) at 25°C, treated with 95°C Trilogy (CMX833-C; Cell Marque, Rocklin, CA) antigen retrieval reagent for 30 minutes, and blocked with Rodent Block M (RBM96; BioCare Medical, Concord, CA) for 30 minutes to reduce nonspecific binding. Retinal whole mounts were then immunostained and flat-mounted on a glass slide with 4′,6-diamidino-2-phenylindole, dilactate (DAPI) Vectashield (Vector, Burlingame, CA) and a coverslip. A goat-anti-Brn3b primary antibody (Santa Cruz Biotechnology, Santa Cruz, CA) was diluted at 1:100 in PBS containing 0.5% Triton X-100 (IB07100; Shelton Scientific, Shelton, CT). A donkey-antigoat Cy3 (#711-166-152; Jackson Laboratories, West Grove, PA) was diluted at 1:250 in PBS. Retinas were incubated for 72 hours at 4°C with primary antibody, washed with PBS, incubated for 72 hours at 4°C with secondary antibody, washed with PBS, and mounted onto glass coverslips using DAPI Vectashield (Vector). Control samples received PBS without primary antibody. Confocal microscopy images were obtained with a Leica TCP SP5 spectral confocal microscope (Leica, Exton, PA) (×63, water-immersion, 1.2 numerical aperture objective). Examples of Brnrb-positive RGCs are shown in the inset of Figure 3. One sample for each retinal quadrant in the proximity of the optic nerve head was analyzed, and all Brn3b-positive RGCs were counted to calculate cell density. To have an approximate measure of the nucleus area, the shorter (S) and the longer (L) diameters were manually identified and the nucleus area was calculated as $\pi \times \frac{1}{2}$ L × ½ S for all Brn3b-positive RGCs in each confocal image.

Western Blotting

At the 4-month end point, eyes were harvested, and retinas of SC-lesioned mice ($n = 5$) were individually dissected and homogenized. Six retinas of unlesioned mice were pooled and homogenized in a single control sample. The total protein was electrophoresed on 10% NuPage gel (Invitrogen, Carlsbad, CA). Western blot using anti-BDNF antibodies (1 mg/mL; ABCAM, Cambridge, MA) detected a single band of approximately 27 kDa, corresponding to BDNF. Immunostaining using anti–β-actin (200 μg/mL; Santa Cruz Biotechnology) detected a single band of approximately 42 kDa, corresponding to β-actin (example in Fig. 4). BDNF and β-actin bands were quantified using ImageJ software for gel densitometry (provided in the public domain by the National Institutes of Health, http://rsbweb.nih.gov/ij/download.html). BDNF protein levels were normalized to the levels of β-actin (BDNF/β-actin) within each sample. Two gel runs were performed and the BDNF/β-actin ratios were averaged and compared with those of controls. The mean value for the control eyes was set at 1.0.

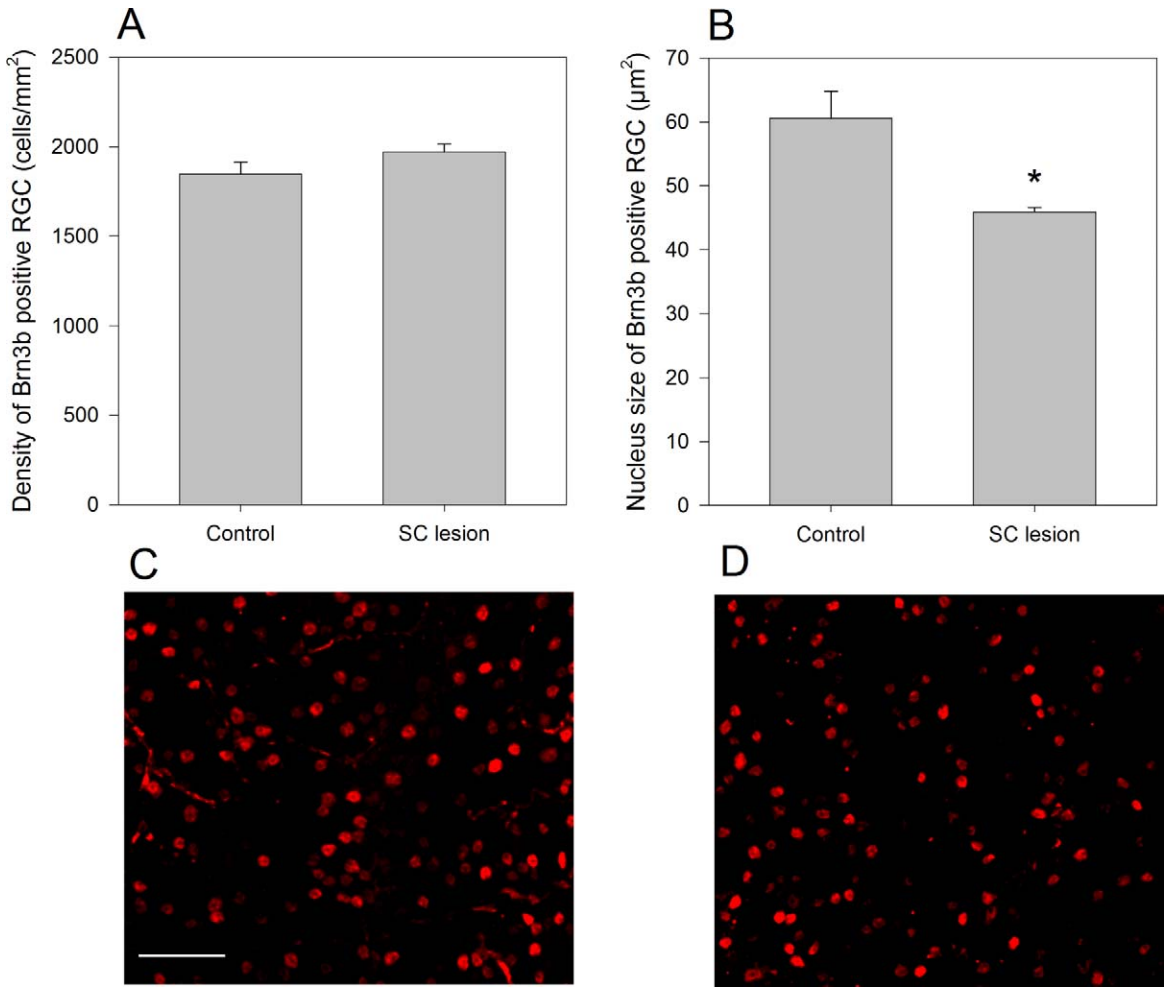

Figure 3. Cell density (**A**) and nucleus size (**B**) of Brn3b-positive RGCs obtained in control retinas and in retinas of eyes that had their contralateral SC lesioned 4 months earlier. *Error bars* represent the SEM ($n = 6$). The *asterisk above the bars* represents the level of significance compared with baseline ($^*P < 0.05$). (**C**, **D**) representative examples of Brn3b-positive RGCs in control (**C**) and SC-lesioned retinas (**D**). The *calibration bar* in (**C**) represents 50 μm.

Results

SC Lesion Induces Rapid, Chronic Loss of PERG Signal

The effects of unilateral SC lesion on the contralateral PERG signal are summarized in Figure 1. The mean PERG amplitude was reduced by more than 60% within 1 day after lesion compared with baseline, and remained reduced to approximately the same level thereafter over 120 days. The effect was highly significant (ANOVA, $P < 0.01$). All postlesion PERG amplitudes were significantly lower than the baseline value (Bonferroni post hoc *t*-tests, *P* values ranging between <0.02 and <0.001).

SC Lesion Induces Delayed, Chronic Loss of OCT-Determined Inner Retinal Thickness

SC-induced changes in retinal thickness are summarized in Figure 2. Although no significant changes occurred in the outer retina over the 4-month observation period (ANOVA, $P = 0.6$), significant thinning occurred in the inner retina (ANOVA, $P < 0.001$). Significant inner retina thinning started 10 days after lesion (Bonferroni post hoc *t*-test, $P < 0.01$) and remained at a level approximately 8 μm thinner than the baseline over the remaining observation period ($P < 0.01$). Ninety-five days after SC, RNFL thickness tended to be slightly thinner (3 μm) compared with baseline, but the difference was not significant ($P = 0.17$).

SC Lesion Is Not Associated with RGC Death

As shown in Figure 3A, Brn3b-positive RGC densities were similar in control mice and in mice whose SC was lesioned 4 months earlier (*t*-test, $P = 0.38$, $n = 6$ for both groups). The RGG nucleus size in SC-lesioned retinas ranged from 44.7 to 46.9 μm^2 as opposed to 46.2 to 66.3 μm^2 in unlesioned retinas. The mean nucleus area (Fig. 3B) was significantly smaller (−24%) in SC-lesioned mice compared with controls (*t*-test, $P = 0.0180$, $n = 6$ for both groups).

BDNF Is Overexpressed in Retinas Contralateral to the Lesioned SC

BDNF immunoblotting of retinas contralateral to the lesioned SC detected a single band of approximately 27 kDa, which in all samples was systematically larger and denser than that of the pooled sample of unlesioned control retinas (Fig. 4). Quantitative densitometry of BDNF bands and normalization to corresponding densitometry of β-actin bands (approximately 42 kDa) indicated that BDNF was overexpressed in retinas of

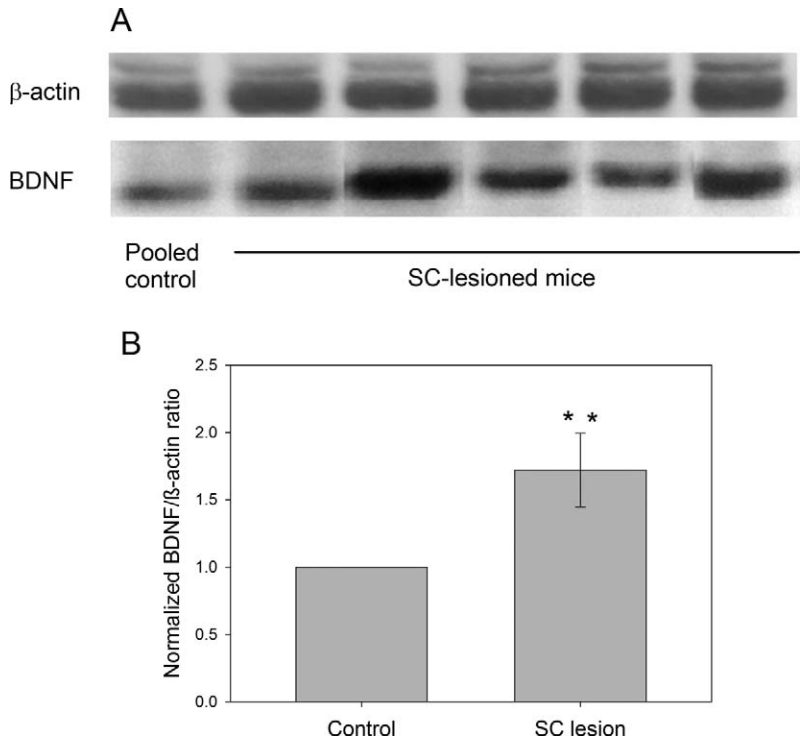

Figure 4. Increase in retinal BDNF expression in response to aspiration of the superficial layers of the contralateral SC 4 months earlier. Western blot analysis was conducted on individual retinal homogenates ($n = 5$) and compared with one homogenate of pooled control retinas ($n = 6$). (**A**) Western blots of BDNF compared with β-actin control. (**B**) Normalized BDNF/β-actin ratios obtained by densitometric analysis in pooled control retinas and in retinas of SC-lesioned mice. *Double asterisks above the right bar* indicate that in SC-lesioned retinas, BDNF was significantly overexpressed ($P < 0.01$). *Error bars* represent the ±95% confidence limits of the mean.

SC-lesioned retinas by a factor of approximately 1.7 compared with unlesioned retinas ($P < 0.01$).

The Effects of SC Lesion Are Specific to RGCs

As a control that chronic SC lesion did not induce generalized retinal dysfunction, we recorded the FERG, a signal known to be generated in the outer retina.[18] After 4 months, the FERG amplitude was not significantly different (–16%) from the baseline ($P = 0.2$, $n = 5$). As a control that the surgical procedure did not cause generalized effects, we recorded the PERG in sham-operated mice, in which only the cortical layers overlying the SC were aspirated. The mean PERG amplitude in sham-operated mice was not significantly different (+7.9%) from the baseline ($P = 0.72$, $n = 6$).

Discussion

The primary goal of this study was to establish the groundwork for a reliable model of inducible, chronic RGC dysfunction not associated with RGC death that could be monitored with noninvasive tools for translational purposes. Aspiration of the superficial layers of the SC resulted in rapid (within 1 day) loss of PERG signal (approximately 60%) that remained at an approximately similar level over an observation period of 4 months. At the 4-month end point, the density of Brn3b-positive RGCs was normal, but their nucleus size was reduced by approximately 24%. Serial OCT measurements showed thinning of the inner, but not outer, retina by approximately 9% starting 10 days after lesion. However, the OCT-measured RNFL thickness at the end point was not different from baseline. Altogether, unchanged Brn3b counts and RNFL thickness suggest that SC lesion did not induce death of RGCs and their intraretinal axons 4 months after lesion. We cannot exclude that subtle axonal changes might have occurred in the proximal optic nerve as it has been reported in a DBA/2J mouse with early glaucoma but with still normal NeuN-labeled RGC counts.[3] We also cannot exclude that significant RGC death might have occurred for an observation period longer than 4 months.

Recent results of our group in mice[19] showed that rapid, dramatic losses of PERG signal (≥50%) can be induced in a reversible manner by means of injections of lidocaine, either retrobulbar or intracollicular. As lidocaine is known to inhibit axon transport, it was suggested that retrograde transport of target-derived material was necessary to sustain RGC electrical responsiveness. In the present study, the main target of the RGC axon was surgically removed, thereby chronically depriving RGC of the main source of target-derived material, which includes neurotrophic factors.[20] The increased BDNF overexpression we found at the end point is consistent with this hypothesis, and can be explained by a compensatory adaptation to chronic deficiency of target-derived neurotrophic factors. It should be taken into account that SC lesion did not inhibit retrograde transport from other areas of RGC projections, including the dorsal lateral geniculate nucleus and the suprachiasmatic nucleus. These additional sources of target-derived neurotrophic factors, together with the retinal BDNF upregulation we documented, were probably sufficient to prevent RGC death.[21] However, the overall deficiency of neurotrophic factors may have caused shrinkage of RGCs and their dendrites, resulting in reduction of nucleus size and inner retina thickness.

Lesions to the SC have been previously shown to cause conspicuous RGC degeneration in neonatal rats. In adult rats, however, SC ablation does not induce significant RGC

degeneration even after many months.[21,22] However, retrograde RGC death after cortical lesions has been reported in adult primates.[23]

What caused reduction of RGC electrical responsiveness in SC-lesioned mice? A possible candidate may be the target-derived BDNF, as it has been shown to induce rapid changes in neuronal excitability even at very low concentrations.[24–26] RGC shrinkage may have also contributed to alter dendritic connectivity.

In conclusion, SC lesion in adult mice results in a rapid, chronic loss of RGC electrical responsiveness that is followed by cell shrinkage but not cell death. The SC-lesion mouse represents a new, inducible model that allows investigating stages and mechanisms of RGC dysfunction per se, dissociated from the confounding effects of cell death that are common in the existing models of optic neuropathies and optic nerve lesions. Cellular dysfunction associated with shrinkage is a common condition in many neurodegenerative disorders of the brain. As the SC-lesion mouse model we have described shares key hallmarks of these conditions, it may provide an opportunity to systematically test the effect of neuroprotective drugs to prevent RGC dysfunction and atrophy using readily available, in vivo longitudinal outcome measures, such as PERG and OCT. Importantly, PERG amplitude losses and recovery have been recently shown to be associated with RGC neurite retraction and growth, respectively, in a mouse model of multiple sclerosis.[27] PERG amplitude losses have been also shown to recover after either IOP lowering in glaucoma[6,28–31] or removal of pituitary tumors.[32] SC lesion in mice using tissue aspiration is a simple, reproducible, well-tolerated procedure that is part of the ordinary armamentarium of the experimental laboratory. Altogether, the SC-lesion mouse model appears to be an attractive translational tool. Future molecular and morphological studies will be needed to further characterize the changes of RGC and their dendrites/axons associated with SC lesions.

Acknowledgments

We thank Rong Weng, MD, PhD, for his help with BDNF immunoblotting and Gus Munguba, PhD, for his help with Brn3b immunohistochemistry.

References

1. Levkovitch-Verbin H. Animal models of optic nerve diseases. *Eye*. 2004;18:1066–1074.
2. Pang IH, Clark AF. Rodent models for glaucoma retinopathy and optic neuropathy. *J Glaucoma*. 2007;16:483–505.
3. Buckingham BP, Inman DM, Lambert W, et al. Progressive ganglion cell degeneration precedes neuronal loss in a mouse model of glaucoma. *J Neurosci*. 2008;28:2735–2744.
4. Howell GR, Libby RT, Jakobs TC, et al. Axons of retinal ganglion cells are insulted in the optic nerve early in DBA/2J glaucoma. *J Cell Biol*. 2007;179:1523–1537.
5. Saleh M, Nagaraju M, Porciatti V. Longitudinal evaluation of retinal ganglion cell function and IOP in the DBA/2J mouse model of glaucoma. *Invest Ophthalmol Vis Sci*. 2007;48:4564–4572.
6. Nagaraju M, Saleh M, Porciatti V. IOP-dependent retinal ganglion cell dysfunction in glaucomatous DBA/2J mice. *Invest Ophthalmol Vis Sci*. 2007;48:4573–4579.
7. Porciatti V, Nagaraju M. Head-up tilt lowers IOP and improves RGC dysfunction in glaucomatous DBA/2J mice. *Exp Eye Res*. 2010;90:452–460.
8. Porciatti V, Pizzorusso T, Cenni MC, Maffei L. The visual response of retinal ganglion cells is not altered by optic nerve transection in transgenic mice overexpressing Bcl-2. *Proc Natl Acad Sci U S A*. 1996;93:14955–14959.
9. Porciatti V, Saleh M, Nagaraju M. The pattern electroretinogram as a tool to monitor progressive retinal ganglion cell dysfunction in the DBA/2J mouse model of glaucoma. *Invest Ophthalmol Vis Sci*. 2007;48:745–751.
10. Yang X, Hernandes MS, Chou T-H, Ruggeri M, Porciatti VA. New mouse model of retinal ganglion cell (RGC) dysfunction: chronic effects of superior colliculus (SC) lesion on inner retina. *ARVO Meeting Abstracts*. 2011;52:4584.
11. Drager UC, Hubel DH. Responses to visual stimulation and relationship between visual, auditory, and somatosensory inputs in mouse superior colliculus. *J Neurophysiol*. 1975;38:690–713.
12. Carpenter P, Sefton AJ, Dreher B, Lim WL. Role of target tissue in regulating the development of retinal ganglion cells in the albino rat: effects of kainate lesions in the superior colliculus. *J Comp Neurol*. 1986;251:240–259.
13. Porciatti V. The mouse pattern electroretinogram. *Doc Ophthalmol*. 2007;115:145–153.
14. Remtulla S, Hallett PE. A schematic eye for the mouse, and comparisons with the rat. *Vision Res*. 1985;25:21–31.
15. Schmucker C, Schaeffel F. A paraxial schematic eye model for the growing C57BL/6 mouse. *Vision Res*. 2004;44:1857–1867.
16. Artal P, Herreros de Tejada P, Munoz Tedo C, Green DG. Retinal image quality in the rodent eye. *Vis Neurosci*. 1998;15:597–605.
17. Porciatti V, Chou TH, Feuer WJ. C57BL/6J, DBA/2J, and DBA/2J. Gpnmb mice have different visual signal processing in the inner retina. *Mol Vis*. 2010;16:2939–2947.
18. Miura G, Wang MH, Ivers KM, Frishman LJ. Retinal pathway origins of the pattern ERG of the mouse. *Exp Eye Res*. 2009;89:49–62.
19. Chou TH, Park KK, Luo X, Porciatti V. Retrograde signaling in the optic nerve is necessary for electrical responsiveness of retinal ganglion cells. *Invest Ophthalmol Vis Sci*. 2013; 54:1236–1243.
20. Almasieh M, Wilson AM, Morquette B, Cueva Vargas JL, Di Polo A. The molecular basis of retinal ganglion cell death in glaucoma. *Prog Retin Eye Res*. 2012;31:152–181.
21. Perry VH, Cowey A. The effects of unilateral cortical and tectal lesions on retinal ganglion cells in rats. *Exp Brain Res*. 1979;35:85–95.
22. Carpenter P, Sefton AJ, Dreher B, Lim W-L. Role of target tissue in regulating the development of retinal ganglion cells in the albino rat: effects of kainate lesions in the superior colliculus. *J Comp Neurol*. 1986;251:240–259.
23. Cowey A, Alexander I, Stoerig P. Transneuronal retrograde degeneration of retinal ganglion cells and optic tract in hemianopic monkeys and humans. *Brain*. 2011;134:2149–2157.
24. Kafitz KW, Rose CR, Konnerth A. Neurotrophin-evoked rapid excitation of central neurons. *Prog Brain Res*. 2000;128:243–249.
25. Kafitz KW, Rose CR, Thoenen H, Konnerth A. Neurotrophin-evoked rapid excitation through TrkB receptors. *Nature*. 1999;401:918–921.
26. Blum R, Kafitz KW, Konnerth A. Neurotrophin-evoked depolarization requires the sodium channel Na(V)1.9. *Nature*. 2002;419:687–693.
27. Enriquez-Algeciras M, Ding D, Mastronardi FG, Marc RE, Porciatti V, Bhattacharya SK. Deimination restores inner retinal visual function in murine demyelinating disease [published online ahead of print January 2, 2013]. *J Clin Invest*. doi: 10.1172/JCI64811.
28. Nesher R, Trick GL, Kass MA, Gordon MO. Steady-state pattern electroretinogram following long term unilateral administration of timolol to ocular hypertensive subjects. *Doc Ophthalmol*. 1990;75:101–109.

29. Colotto A, Salgarello T, Giudiceandrea A, et al. Pattern electroretinogram in treated ocular hypertension: a cross- sectional study after timolol maleate therapy. *Ophthalmic Res*. 1995;27:168–177.
30. Ventura LM, Porciatti V. Restoration of retinal ganglion cell function in early glaucoma after intraocular pressure reduction: a pilot study. *Ophthalmology*. 2005;112:20–27.
31. Sehi M, Grewal DS, Goodkin ML, Greenfield DS. Reversal of retinal ganglion cell dysfunction after surgical reduction of intraocular pressure. *Ophthalmology*. 2010;117:2329–2336.
32. Ventura LM, Venzara FX III, Porciatti V. Reversible dysfunction of retinal ganglion cells in non-secreting pituitary tumors. *Doc Ophthalmol*. 2009;118:155–162.